Variations in Cathodoluminescent Intensity of Spacecraft Materials Exposed to Energetic Electron Bombardment

Justin Dekany[1], Justin Christensen[1], JR Dennison[1], Amberly Evans Jensen[1], Gregory Wilson[1], Todd Schneider,[2] Charles W. Bowers[3] and Robert Meloy[4]

[1]Utah State University, [2]NASA Marshall Space Flight Center, [3]NASA Goddard Space Flight Center, [4]ASRC Federal Space and Defense Inc.

13th Spacecraft Charging Technology Conference SCTC 2014

Utah State University MATERIALS PHYSICS GROUP

Abstract

Many contemporary spacecraft materials exhibit cathodoluminescence when exposed to electron flux from the space plasma environment. A quantitative, physics-based model has been developed to predict the intensity of the glow as a function of incident electron current density and energy, temperature, and intrinsic material properties. We present a comparative study of the absolute spectral radiance for several types of dielectric and composite materials based on this model which spans three orders of magnitude. Variations in intensity are contrasted for different electron environments, different sizes of samples and sample sets, different testing and analysis methods, and data acquired at different test facilities. Together, these results allow us to estimate the accuracy and precision to which laboratory studies may be able to determine the response of spacecraft materials in the actual space environment. It also provides guidance as to the distribution of emissions that may be expected for sets of similar flight hardware under similar environmental conditions.

Test Methods and Facilities

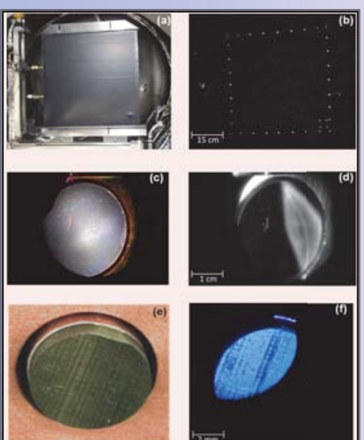

Sample images in ambient light (left) and under electron bombardment (right) showing variations in sample composition, size and facility.

- ❑ (a-b) 41x41 cm sample of carbon-loaded polyimide mounted in the MSFC test chamber, with 36 epoxy glue dots luminescing under electron flux.
- ❑ (c-d) 2.5 cm diameter sample of thin disordered SiO_2 coating on Au-coated mirror mounted in the USU SEEM test chamber. (d) Image with the beam focus adjusted so that electrons impinge and cathodoluminescence is evident only on the right side of the sample.
- ❑ (e-f) 1 cm diameter sample of cyanate ester/graphite fiber composite at USU. Striations in the images result from the composite fiber structure of the material. (f) Image with the electron beam offset to the top left, limiting cathodoluminescence to this quadrant.
- ❑ (b) and (d) are CCD video frame images; all other images are SLR still color photographs.

References

[1] J.R. Dennison, A.E. Jensen, J. Dekany, G. Wilson, C.W. Bowers and R. Meloy, "Diverse Electron-induced Optical Emissions from Space Observatory Materials at Low Temperatures," *Proc. SPIE Cryogenic Optical Systems and Instr. Conf.*, Vol. 8863, 2013, pp. 88630B1-88630B15.

[2] D.C. Ferguson, J.-M. Krezan, D.A. Barton, J.R. Dennison, and S. Gregory, "On the Feasibility of Detecting Spacecraft Charging and Arcing by Remote Sensing," *J. Spacecraft and Rockets*, 2014, in press.

[3] A.E. Jensen, J.R. Dennison, G. Wilson, J. Dekany, C.W. Bowers, R. Meloy and J.B. Heaney, "Properties of Cathodoluminescence for Cryogenic Applications of SiO_2-based Space Observatory Optics and Coatings," *Proc. SPIE Cryogenic Optical Systems and Instr. Conf.*, Vol. 8863, 2013, pp. 88630A1-88630A10.

[4] A.E. Jensen and J.R. Dennison, "Defects Density of States Model of Cathodoluminescent Intensity and Spectra of Disordered SiO_2," *Proc. 13th Spacecraft Charging Techn. Conf.*, (Pasadena, CA, June, 2014).

[5] J.R. Dennison, J. Dekany, J.C. Gillespie, P. Lundgreen, A. Anderson, A.E. Jensen, G. Wilson, A.M. Sim, and R. Hoffmann, "Synergistic Models of Electron Emission and Transport Measurements of Disordered SiO_2," *Proc. 13th Spacecraft Charging Techn. Conf.*, (Pasadena, CA, June, 2014).

[6] G. Teyssedre, J. Franceschi, and C. Laurent, "Cathodo-and electro-luminescence spectra in insulating polymers: a parallel approach for inferring electrical ageing mechanisms." *Proc. IEEE-CEIDP*, pp. 824-827, 2007.

[7] G. Teyssedre, C. Laurent, G.C. Montanari, F. Palmieri, A. See, L.A. Dissado and J.C. Fothergill, "Charge distribution and electroluminescence in cross-linked polyethylene under dc field," J. Phys. D: Appl. Phys., **34,** 2830, 2001.

[8] H.-J. Fitting, T. Barfels, A. von Czarnowski, and A. N. Trukhin, "Electron Beam Induced Optical and Electronical Properties of SiO_2," Materials Science and Engineering, **B71**, 109-114 (2000).

[9] A.E. Jensen, J.R. Dennison, G. Wilson, and J. Dekany, "Nanodielectric Properties of High Conductivity Carbon-Loaded Polyimide Under Electron-Beam Irradiation," *Proc. 2013 IEEE Intern. Conf. on Solid Dielectrics (ICSD)*, (Bologna, Italy, June, 2013), pp.730-735.

[10] A.M. Sim and J.R. Dennison, "Comprehensive Theoretical Framework for Modeling Diverse Electron Transport Experiments in Parallel Plate Geometries," Paper Number, AIAA-2013-2827, *5th AIAA Atmospheric and Space Environ. Conf.*, (San Diego, CA, June, 2013).

[11] J. R. Dennison, A. Evans, G. Wilson, J. Dekany, C. W. Bowers, and R. Meloy, "Electron Beam Induced Luminescence of SiO_2 Optical Coatings," Proc. IEEE-CEIDP (2012).

[12] J.A Roth, R. Hoffmann, and J.R. Dennison, "Effects of Radiation Induced Conductivity on Electrostatic Discharge in Insulating Materials," *Proc. 1st AIAA Atmospheric and Space Environments Conf.* (San Antonio, TX, 2009).

[13] J. Christensen, J. Dekany, and J.R. Dennison, "Stochastic Variations of Cathodoluminescent Intensity of Bisphenol/Amine Epoxy Exposed to Energetic Electron Bombardment," Utah State University Student Showcase, Logan, UT, April, 2014.

[14] G. Wilson and J.R. Dennison, "Approximation of Range in Materials as a Function of Incident Electron Energy," *IEEE Trans. on Plasma Sci.*, **40**(2), 305-310 (2012).

[15] W.Y. Chang, J.R. Dennison, N. Nickles and R.E. Davies, "Utah State University Ground-based Test Facility for Study of Electronic Properties of Spacecraft Materials," *Proc. 6th Spacecraft Charging Techn. Conf.*, (AFRL Sci. Center, Hanscom Air Force Base, MA, 2000).

[16] J. Dekany, R.H. Johnson, G. Wilson, A. Evans and J.R. Dennison, "Ultrahigh Vacuum Cryostat System for Extended Low Temperature Space Environment Testing," *Proc. 12th Spacecraft Charging Techn. Conf.*, (Kitakyushu, Japan, May, 2012).

[17] C. Leinert, *et al.*, "The 1997 Reference of Diffuse Night Sky Brightness," Astron. Astrophys. Suppl. Ser., **127**, 1, 1997.

[18] K. Peterson and J.R. Dennison, "Atomic Oxygen Modification of the Nanodielectric Surface Composition of Carbon-Loaded Polyimide Composites," Am. Phys. Soc. Four Corner Section Meeting, Denver, CO, October, 2013.

Many members of the USU Materials Physics Group have contributed to the collective work which made this summative paper possible. Discussions with the James Webb Space Telescope Spacecraft Charging Working Group have been most helpful in formulating the ideas presented here. We gratefully acknowledge Michael Taylor for the use of infrared and CCD video cameras.

← Scan for USU Materials Physics Group References

Model of Cathodoluminescent Intensity

The model developed for the observed electron-induced luminescence phenomenon is based on band theory of highly disordered insulating materials [3,7,10]. The observed luminescence occurs when an incident high energy, charged particle undergoes a series of inelastic collisions exciting valence band electrons into the conduction band. The excited electrons rapidly decay to localized (shallow trapped) states, with a mean binding energy ε_{ST} below the mobility edge. A final electron transition, from the short-lived shallow trap states to longer-lived deep trap states is the origin of the emitted photon.

The model predicts that the overall luminescencent intensity:

$$I_\gamma(J_{inc},E_{inc},T,\lambda) \propto \frac{\dot{D}(J_{inc},E_{inc})}{\dot{D}+\dot{D}_{sat}}\left\{\left[e^{-(\varepsilon_{ST}/k_BT)}\right]\left[1-e^{-(\varepsilon_{ST}/k_BT)}\right]\right\}\times\left\{\left[1-\mathbb{A}_f(\lambda)\right]\left[1+\mathbb{R}_m(\lambda)\right]\right\} \qquad \text{Eq. (1)}$$

The dose rate $\dot{D}$ (absorbed power per unit mass) is given by

$$\dot{D}(J_{inc},E_{inc}) = \frac{J_{inc}E_{inc}[1-\eta(E_{inc})]}{q_e\rho_m}\times\begin{cases}[1/L] & ;\ R(E_{inc})<L\\ [1/R(E_{inc})] & ;\ R(E_{inc})>L\end{cases}. \qquad \text{Eq. (2)}$$

J_{inc}, incident current density,
E_{inc}, incident beam energy
T, temperature
L, sample thickness
λ, photon wavelength
q_e, electron charge,
ρ_m, mass density of the material
$\eta(E_b)$, contribution of backscattered yield
$\dot{D}_{sat}$, material-dependent saturation dose rate

The exponential terms in Eq. (1) account for temperature dependence [3]. The last two λ-dependant terms correct for photon absorption within the luminescent material and reflection from any underlying coating [11]. A more detailed discussion of the model is given in [1]. This work focuses on the dependence of spectral radiance on J_{inc}, E_{inc}, and the range of the deposited electrons, $R(E_{inc})$.

The dependence of the spectral radiance on incident current density, J_{inc}, in Eq.(1) is through the dependence on dose rate; $I_\gamma(J_{inc}) \propto \dot{D}(J_{inc})/[D(J_{inc})+\dot{D}_{sat}] \propto J_{inc}/[J_{inc}+J_{sat}]$.

- At low dose rates ($\dot{D} \ll \dot{D}_{sat}$), I_γ is linearly proportional to J_{inc}.
- At higher current densities ($\dot{D} \gg \dot{D}_{sat}$), saturation occurs when trap states fill, limiting the number of states electrons can decay into; I_γ approaches a constant material-specific saturation intensity.
- Such saturation effects, at increasing current densities and fixed incident energies, have been reported for disordered SiO_2 [3], nanodielectric carbon-loaded polyimide [9], cynate ester/graphite fiber composites [12], and bisphenol/amine epoxy [1,13].

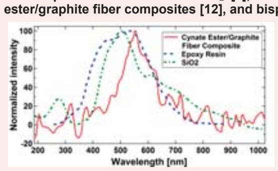

Cathodoluminescent spectra of three highly disordered insulating materials. Shown are: cynate ester/graphite fiber composite at ~100 K (red solid curve) [12], epoxy resin at ~295 K (blue dashed curve) [6], and SiO_2-coated mirror at ~269 K (green dash-dotted curve) [3]. Spectra are normalized at maximum intensities and are not corrected for the wavelength-dependant relative detector sensitivity.

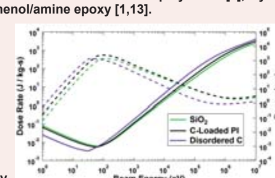

Range (solid curves) and dose rate (dashed curves) of three disordered materials (SiO_2, carbon-loaded polyimide, and graphitic amorphous carbon) as a function of incident electron energy using calculation methods and the continuous slow-down approximation [14].

Variations with Energy and Penetration Depth

The energy dependence of the spectral radiance is more complicated, due to the energy-dependent penetration depth or range, $R(E_{inc})$, in Eq. (2). For nonpenetrating radiation—where the energy-dependent penetration depth or range, $R(E_{inc})$, is less than the film thickness L—all incident power is absorbed in the material. At low incident power, both $\dot{D}$ and I_γ are linearly proportional to the incident energy and power density, $(J_{inc}E_{inc}/q_e)$. At higher incident power, both $\dot{D}$ and I_γ exhibit saturation effects at increasing energy and fixed current density. For penetrating radiation—where $R(E_{inc})>L$—the *absorbed* power is reduced by a factor of $[L/R(E_{inc})]$ [14] leading to a similar dependence for I_γ. Fig. 1 shows the range and dose rate for select disordered materials as functions of incident energy.

An energy-dependent correction to the incident flux, $J_{inc}[1-\eta(E_{inc})]$, is also included in Eq. (2) to account for quasi-elastic backscattered electrons that do not deposit substantial energy; $\eta(E_{inc})$ is the backscattered electron yield [11]. For the most part, this correction is small and weakly dependant on energy. For biased samples, or when excess charge is stored in the trap states, a surface voltage V_s results and E_{inc} is replaced everywhere in Eqs. (1) and (2) by the landing energy, $(E_{inc}-q_eV_s)$.

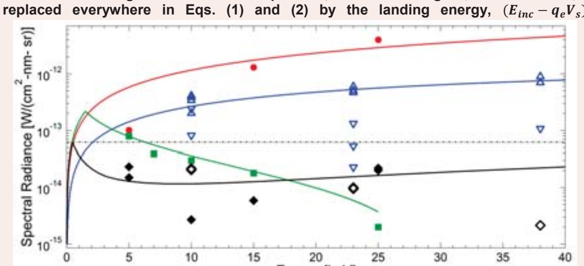

Absolute cathodoluminescent spectral radiance versus incident electron energy of four materials, scaled to 10 nA/cm² electron current density.

❑ The plot shows data for:

- SiO_2-coated mirror (green square) [3,4]
- Cynate ester/C-fiber composite (red circle) [12]
- C-loaded polyimide (black diamonds) [1,9]
- Bisphenol/amine epoxy (blue triangles) [1,13]

❑ Fits are based on Eqs. (1) and (2).

❑ Data were taken with the CCD video camera at USU (solid symbols) and MSFC (open symbols).

❑ The approximate level of the zodiacal background stray light intensity at 863 nm is shown for comparison (dashed grey line) [17].

Variations with Materials

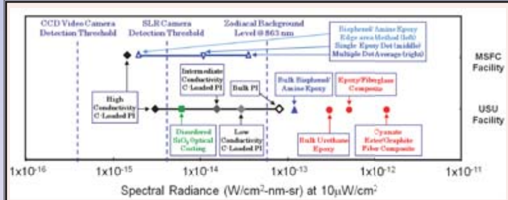

Measured absolute cathodoluminescent intensities for ~10 keV electron bombardment scaled to 10 μW/cm², representative of severe space environments.

❑ The materials shown, in approximate order of increasing intensity, are:

- Three levels of decreasing carbon loading of polyimide from high to low conductivity and bulk polyimide (black squares);
- Disordered SiO_2 optical coatings (green);
- Neat bisphenol/amine and urethane epoxies (blue);
- Composite resin fiber materials including cyanate ester/graphite fiber, urethane epoxy/carbon fiber, and epoxy/fiberglass composites (red).

❑ Measurements at the two test facilities are identified at right.

❑ Three data analysis methods are compared for bisphenol/amine samples; these range over more than two orders of magnitude, illustrating the need for well designed test methods.

❑ Spectral radiance for the zodiacal background stray light intensity at 863 nm is shown for comparison (dashed blue line).

❑ Data acquired using the CCD video camera (863 nm weighted central wavelength and 500 nm bandwidth); the detection thresholds of the cameras at the MSFC facility [1].

Variations in Analysis Methods

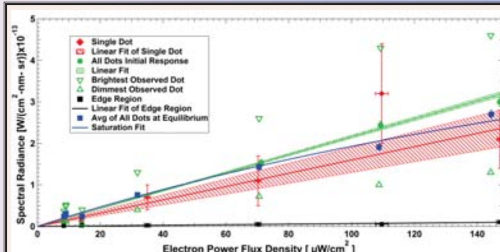

Comparison of different methods to determine the absolute spectral radiance per incident electron power density as a function of incident electron energy for bulk bisphenol/amine epoxy samples.

❑ The slope of the linear fit, or conversion efficiency of high energy electron power to luminescent photon power, of 2.16 x 10^{-9} [W/(W-nm-sr)] (±2%) determined from the statistical analysis of 36 "glue dot" (green) is ~35% larger than from analysis of a single "glue dot" (red) and ~32X larger than from using edge region analysis (black).

❑ The range of variations of the 36 sample data set is indicated by the ~±5% standard deviation (error bars) and ~±60% minimum to maximum range (green triangles). Errors for the spectral radiance and slope values for the linear fit of the single "glue dot" are ~5X large than for the analysis of all dots.

❑ Comparison for the multiple sample data set of green initial (unsaturated) and blue equilibrium (saturated) curves show saturation effect at higher dose rates. The fit for the saturated (blue) curve from Eq. (1) is of the form , with a proportionality constant of $9\cdot10^{-13}$[W/(cm²nm·sr)] (±20%) and D_{sat}=1.5 kGy/s (±30%) or P_{sat}=360 μW/cm².

Conclusion

Cathodoluminescence is an important space environment-induced phenomenon to understand, especially in applications where extremely sensitive space-based optical detection is necessary.

❑ Measurements of the absolute spectral intensities per incident electron flux have been presented that confirm a quantitative, physics-based model to predict the intensity of the glow as a function of incident electron current density and energy, temperature, and sample thicknesses and composition.

❑ Comparisons for these materials show three orders of magnitude variation.

❑ For bulk nonpenetrating materials, spectral radiance increases with increasing incident electron power and flux. In thin films where electron penetration is possible, a linear relation is seen at low energies, but once penetration occurs intensity decreases with increasing energies.

❑ Composite materials, where both penetrating and nonpenetrating electrons effects were present, required a combination of these two effects in the model. Saturation effects at higher doses were observed and accurately modeled, for both penetrating and nonpenetrating electrons.

❑ Statistical analysis of the observed statistical fluctuations of cathodoluminescence for a large set of similar epoxy samples exposed simultaneously to similar space-like monoenergetic electron flux conditions provided measures of both the instrumentation precision and the stochastic variations inherent to the material.

❑ The statistical analysis of the combined results of studies of numerous similar samples led to higher precision and accuracy results that allow for quantification of additional more subtle effects.

❑ Together, these results allow us to estimate the accuracy and precision to which laboratory studies may be able to determine the response of spacecraft materials in the actual space environment. It also provides guidance as to the distribution of emissions that may be expected for sets of similar flight hardware under similar environmental conditions.